



Remote Sounding with Advanced Infrared and Microwave Instruments

Chris Barnet
NOAA/NESDIS/STAR

University of Maryland, Baltimore County (Adjunct Professor)

AIRS Science Team Member

NPOESS Sounder Operational Algorithm Team Member

GOES-R Algorithm Working Group – Chair of Sounder Team

NOAA/NESDIS representative to IGCO

Tuesday July 24, 2007

**Workshop on Applications of Remotely Sensed
Observations in Satellite Data Assimilation**



Sounding Theory Notes for the discussion today is on-line

voice: (301)-316-5011

email: chris.barnet@noaa.gov

ftp site: <ftp://ftp.orbit.nesdis.noaa.gov/pub/smcd/spb/cbarnet/>
..or.. [ftp ftp.orbit.nesdis.noaa.gov](ftp://ftp.orbit.nesdis.noaa.gov), [cd pub/smcd/spb/cbarnet](ftp://ftp.orbit.nesdis.noaa.gov/pub/smcd/spb/cbarnet)

Sounding NOTES, used in teaching UMBC PHYS-741: Remote Sounding and UMBC PHYS-640: Computational Physics (w/section on Apodization)

[~/reference/rs_notes.pdf](#)

[~/reference/phys640_s04.pdf](#)

These are *living* notes, or maybe a scrapbook – they are not textbooks.

For an excellent text book on the topic of remote sounding is:

Rodgers, C.D. 2000. Inverse methods for atmospheric sounding: Theory and practice. World Scientific Publishing
238 pgs



Topics for Lectures

- Monday July 23, 2007
 - Introduction to AIRS & IASI and our plans to use *operational* sounders to retrieve atmospheric and surface products.
 - Introduction to Sounding Methodology
 - Cloud clearing
 - Statistical Regression Retrievals
- Tuesday July 24, 2007
 - Sidebar: Comparison of Dispersive and Interferometric Instruments
 - Introduction to Sounding Methodology (continued)
 - The forward model: Converting state vector to radiances.
 - The inverse problem: Converting radiances to a state vector.
- Wednesday July 25, 2007
 - Introduction to Sounding Methodology (continued)
 - Vertical Averaging Kernels & Error Covariance Matrices
 - Validation of Products
 - Atmospheric Carbon Retrievals

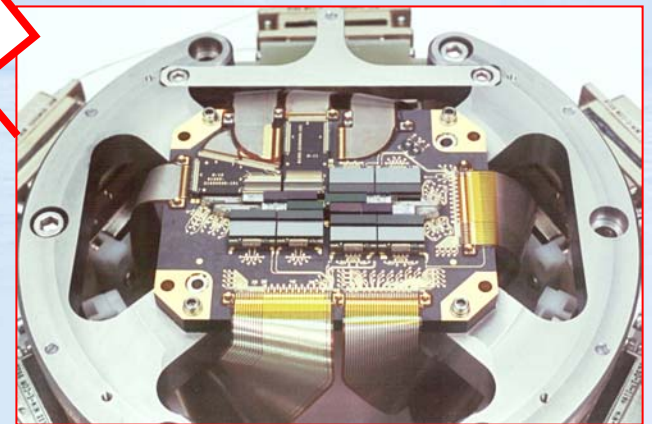
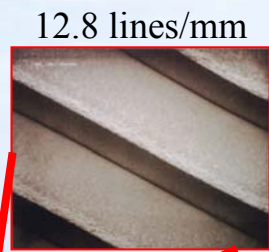
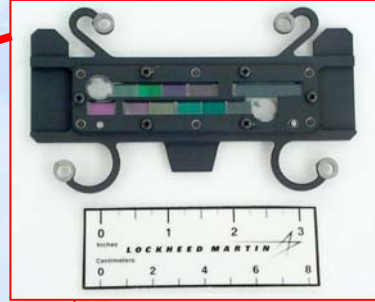
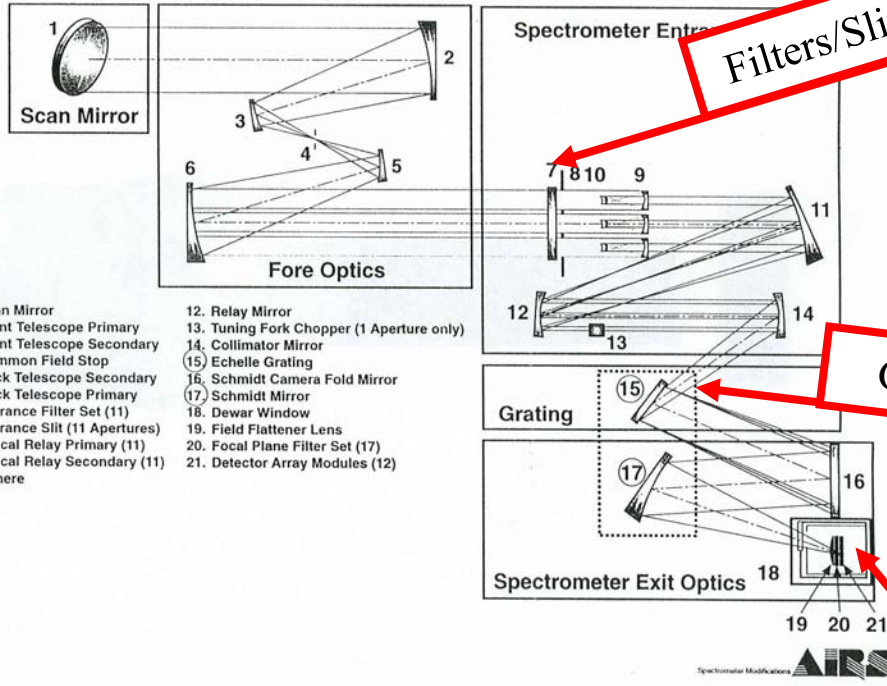


Sidebar:

Comparison of Dispersive and
Interferometric Instruments

(12 Slides)

AIRS Optical Diagram

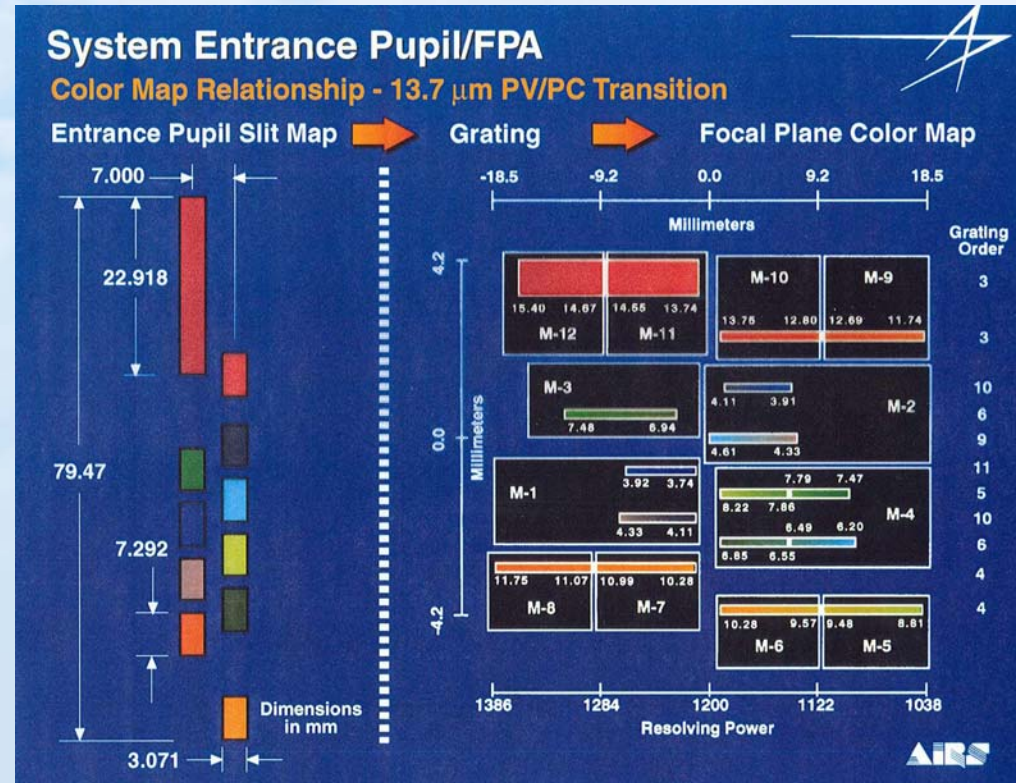


Only moving parts on AIRS are

1. Scan mirror
2. Sterling Cooler Pistons
(mechanical cooler required to cool & control focal plane at 58K)

AIRS Instrument (continued)

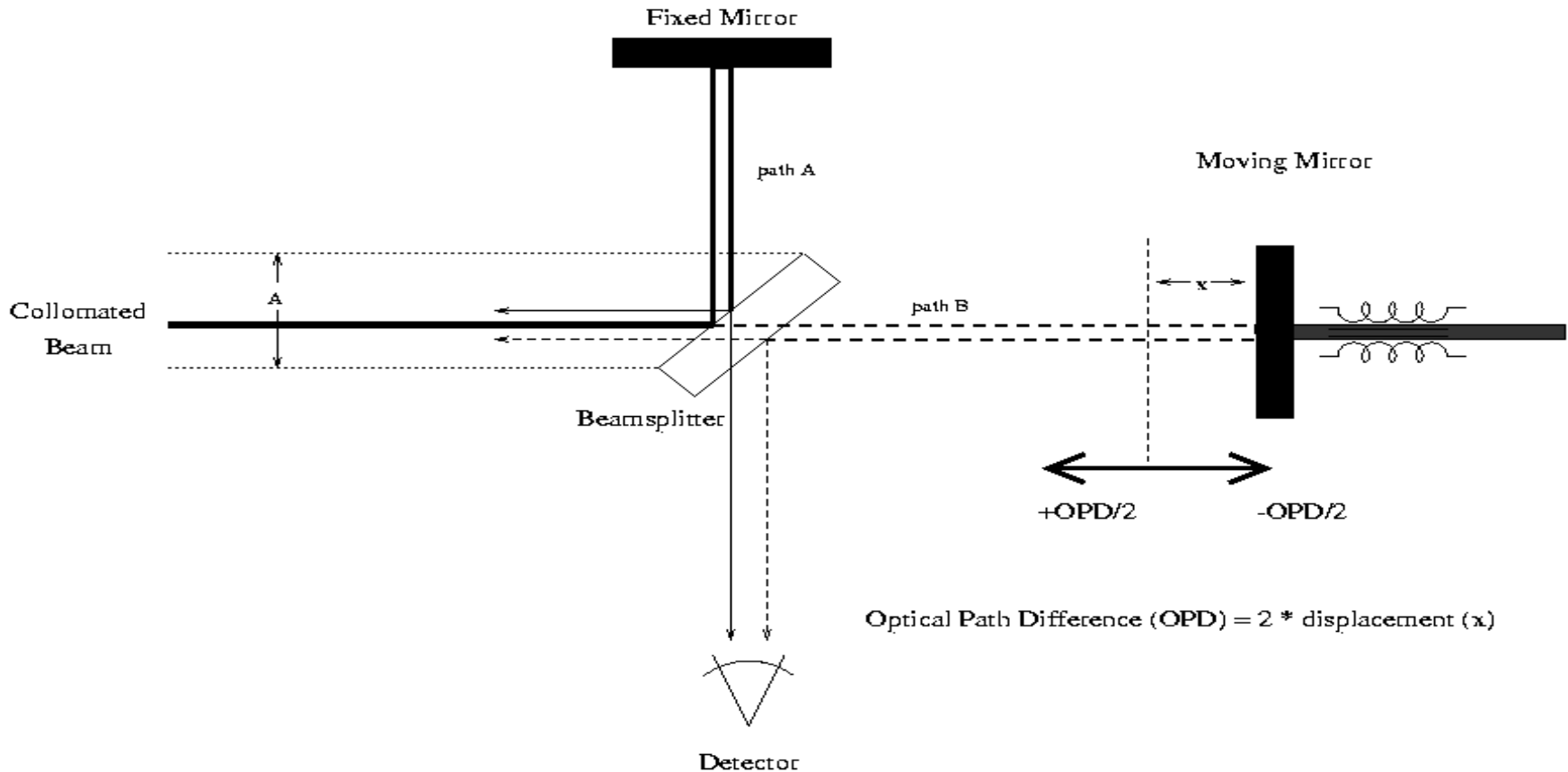
- Entrance Slits, with interference filters to select grating order and to remove stray light, are used to map spectral regions onto focal plane linear arrays.
- Optical design is “pupil imaging” to eliminate spatial sensitivity within a FOV
- Resolving Power is inversely related to slit width $R_{AIRS}=1200$



NOTE: Each detector is $\cong 50 \mu\text{m}$

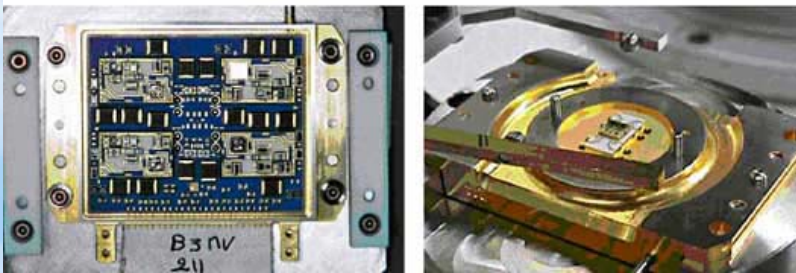
$$R = (FL/W) * \tan(\theta) = 227/3 * \tan(85^\circ)$$

Illustration of a Simplified Michelson Interferometer

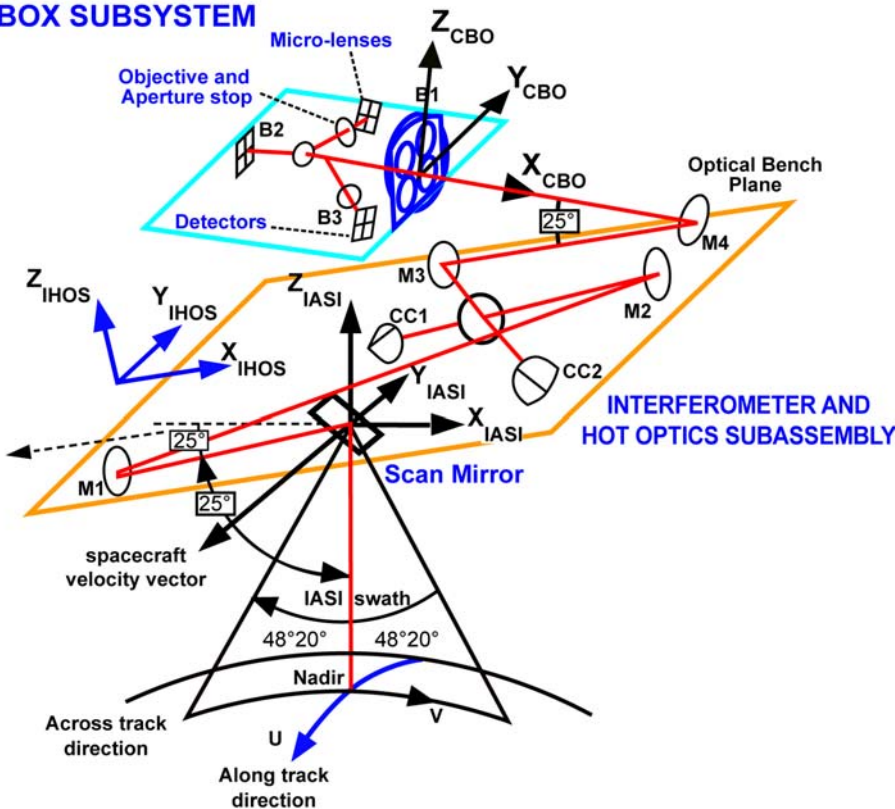


NOTE: The IASI design is much more complex. Mirrors are corner cubes (2 reflections, but very easy/stable to align). Twelve detectors are employed to improve signal-to-noise (3 bands/spectra) and sample 4 FOV's simultaneously.

IASI Optical Diagram



COLD BOX SUBSYSTEM



IASI has 4 FOV's measured simultaneously

Corner cubes are used to maintain alignment in space environment.

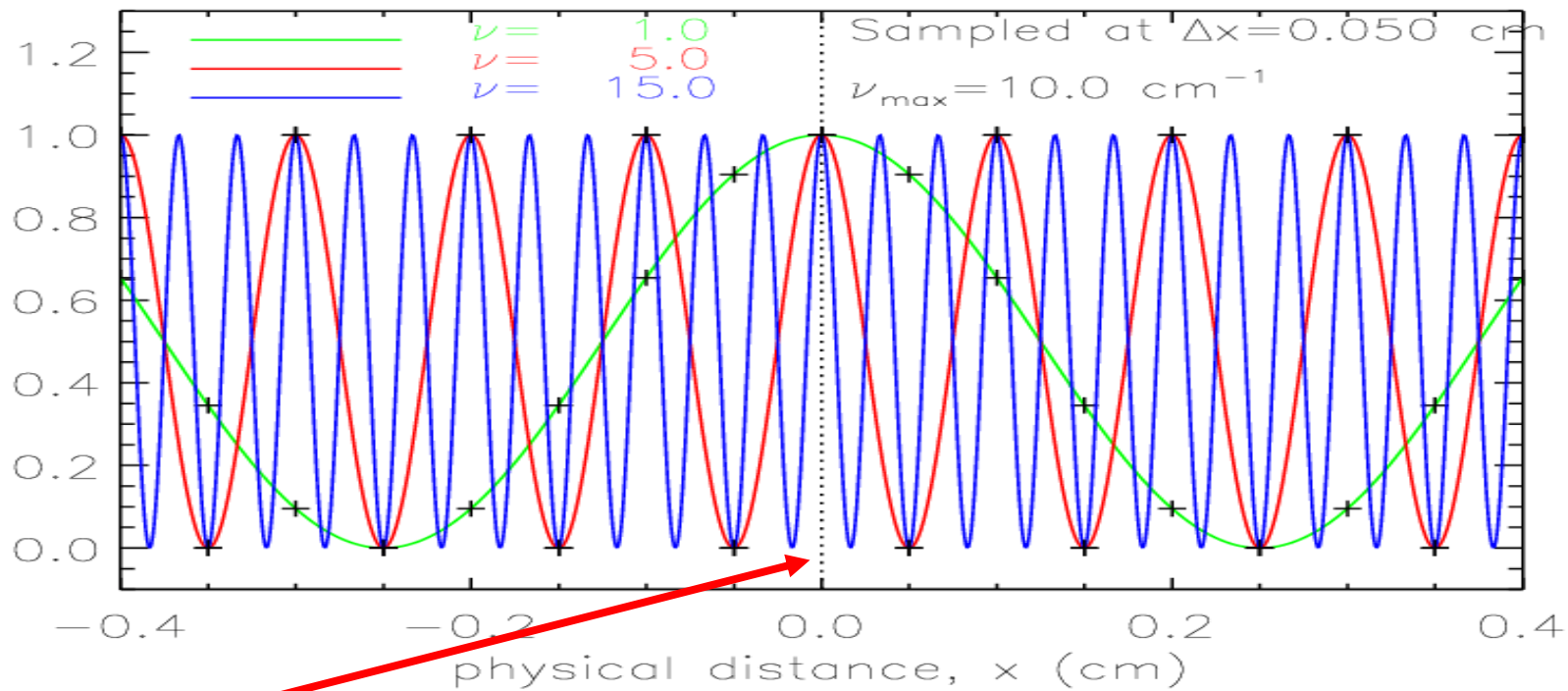
Small number of detectors allows a passive cooler (90 K) can be used.

Moving parts in IASI:

1. Scan mirror
2. Corner Cube (CC1)



Interferometer Measures the Cosine Transform of Radiance

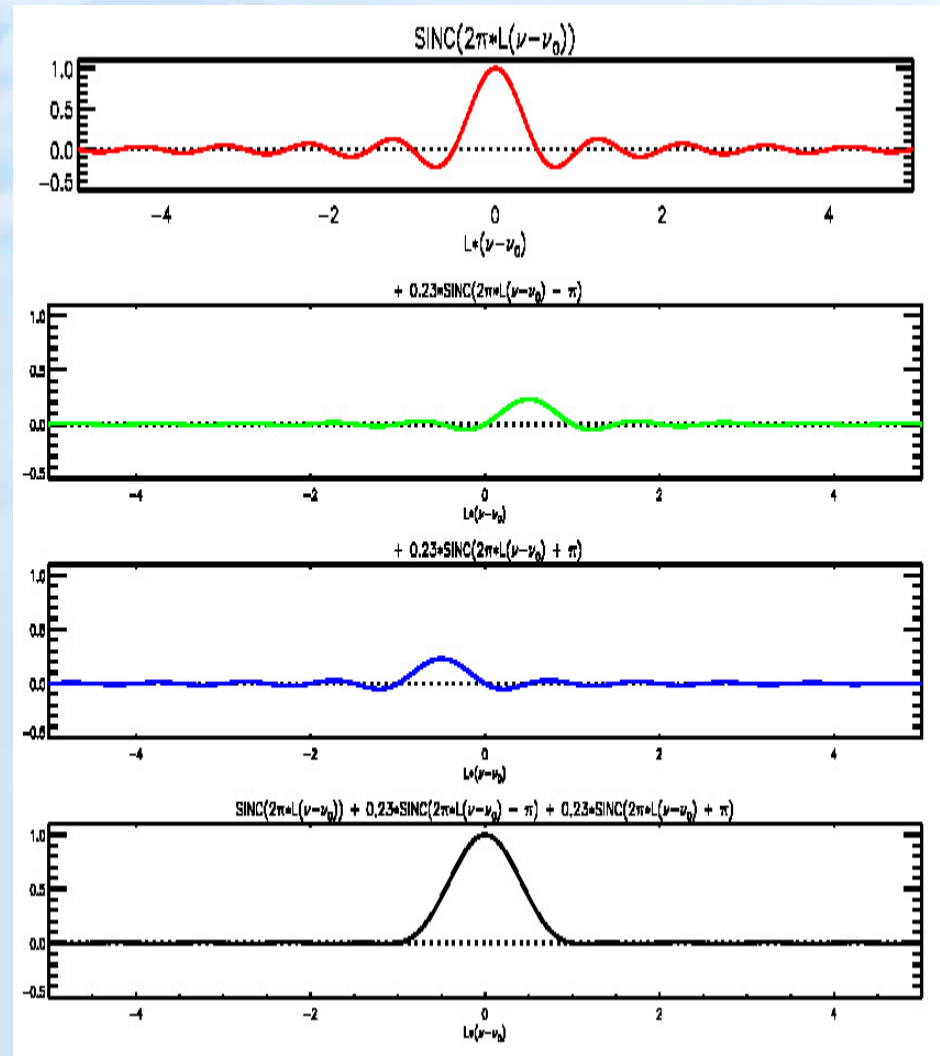


- At $x=0$, a large contribution from all frequencies occurs. The “center burst” is equal to the total radiance within a spectral band.
- At $x \neq 0$, the detector measures the sum of all frequencies in the pass-band. Constructive and destructive interference occurs as a function of OPD .

What is Apodization

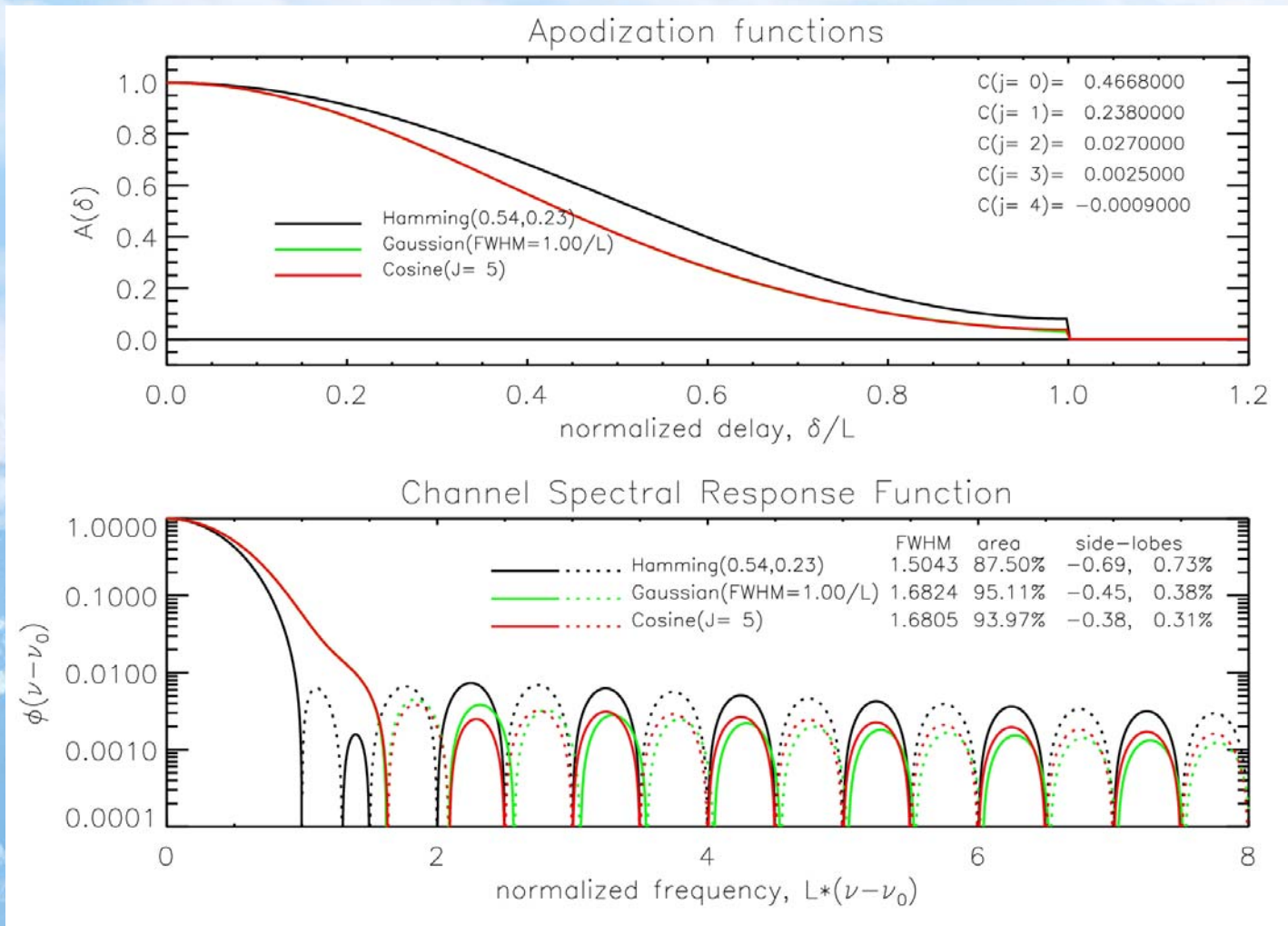
(literal translation is “remove the foot”)

- An apodization function is a multiplied by interferogram.
 - Most interferometers have some amount of “self-apodization” due to change in throughput as the mirror moves.
 - If the apodization function does not have zeroes, then the process is reversible.
- This is equivalent to a running mean in the spectral domain.
- Hamming’s apodization function is a 3-pt weighted running mean.
- Apodization is a trade-off between side-lobes and the width (or area) of the central lobe





IASI Apodization Function is a Truncated Gaussian

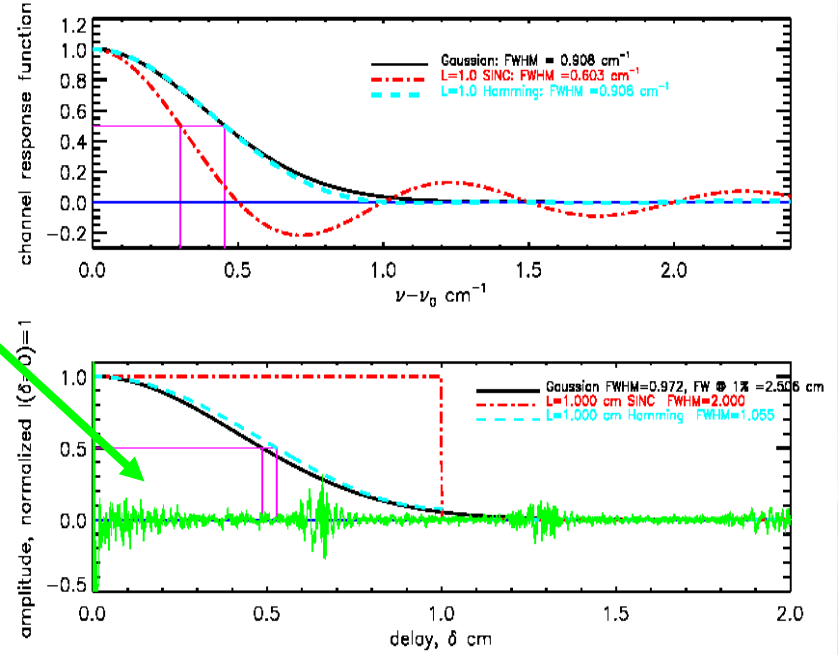


NOTE: Gaussian Apodization DOES NOT Change the Information Content of Radiances



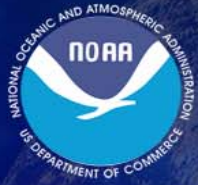
Apodization Alters the ILS and Spectrally Correlates the Noise.

- Interferometers measure interferograms (green curve) signal as a function of optical delay δ
- Performing an inverse cosine transform will yield the spectrum.
- Un-apodized transforms (red) have a $\text{SINC}(x) = \text{SIN}(x)/x$ instrument line shape (ILS).
- AIRS has a Gaussian ILS (black)
- Apodization can produce an ILS that is localized and has small ($< 1\%$) side lobes. But the tradeoff is that the central lobe is wider and the signal is spectrally correlated between neighboring channels



	Gaussian	Hamming	Blackman
FWHM / FWHM(SINC)	1.682	1.5043	1.905
Random Noise reduction	1.735	1.586	1.812
Maximum Side-Lobe	0.45%	0.73%	0.12%
% of signal in central Lobe	95.1%	87.5%	99.8%

Channel Separation	Gaussian	Hamming	Blackman
± 1	70.74%	62.5%	75.5%
± 3	25.0%	13.3%	31.6%
± 4	4.43%	-	6.57%
± 5	0.38%	-	0.53%
± 6	0.025%	-	-



Dispersive versus Interferometer

Dispersive (<i>e.g.</i> , Grating)	Interferometer
Optics are solid state, grating is analogous to a solid state interferometer”	Requires moving mirror that is stable over 150 ms integration time.
Linear arrays w/ read out integrated circuits make a large number of detectors feasible and very fast to read out. Large number of detectors and read out circuits requires cooling.	Multiplex (Fellgett’s) Advantage: all f ’s measured by one detector (rapid sampling in interferogram domain). Each time sample measures entire spectrum.
Detector noise is less sensitive to scene radiance. Focal plane requires cooling to achieve same signal to noise.	Throughput (Jacquinot’s) Advantage: does not require a slit. One half of light strikes detector.
Frequencies are determined by geometry, therefore, instrument must be held constant in temperature. Small remnant frequency drift must be handled in radiative transfer.	Connes Advantage: Mirror distance (determines frequency of channels) can be measured with a reference laser that has a known frequency and is stable – therefore, a standard set of frequencies can be maintained.
Instrument design for multiple FOV’s is too complex; however, low noise means fast integration time and having all FOV’s measured by the same instrument is an advantage.	Multiple FOV’s can be measured simultaneously. Sampling and resolution is determined by optical path and therefore, FOV’s must be
Gratings are constant resolving power, therefore, both sampling and resolution change with frequency, $\Delta\nu = R/\nu$	Continuous spectrum at constant resolution that is Nyquist sampled, $\Delta\nu \cong 0.9/L$



But the Question is Which Approach is Most Suitable for the Space Environment

- All optics must be stable to vibration during integration time
 - AIRS has no moving optical components except the scan mirror (common to all scanning instruments).
 - IASI has corner cube mirror that moves 2 cm in 145 milli-seconds.
 - CrIS has “porch swing” mirror that moves 0.8 cm in 145 milli-seconds.
- Interferometers for Earth applications are passively cooled.
 - Detector responsivity is a non-linear function of temperature and small drifts will make it difficult to calibrate.
- Small drift in reference laser (laser diodes used are sensitive to temperature) makes long-term frequency calibration difficult.
- Interferogram has a large dynamic range and detector response is non-linear, therefore, the interferometer calibration is more complicated.
- Detectors are more sensitive to emissions from optics and spectrometer body and makes calibration more difficult due to phase shifts between scene and instrument.
- Calibration for cold-scenes is difficult, both due to non-linearity issues, and corrections for phase shift (instrument emission begins to dominate).

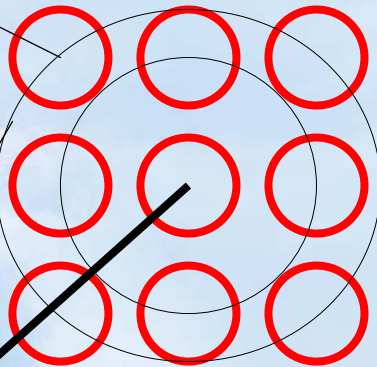
Interferometer: Sub-pixel FOV Issue

- Spectral resolution and ILS are defined by maximum optical path difference

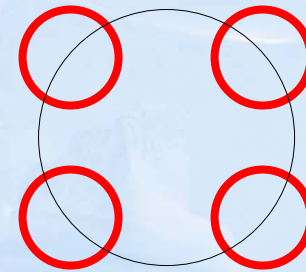
Largest Optical Path Difference

NOTE: Nyquist sampled, can be mathematically re-sampled to a smaller OPD.

CrIS
(14 km FOV's)



IASI
(12 km FOV's)



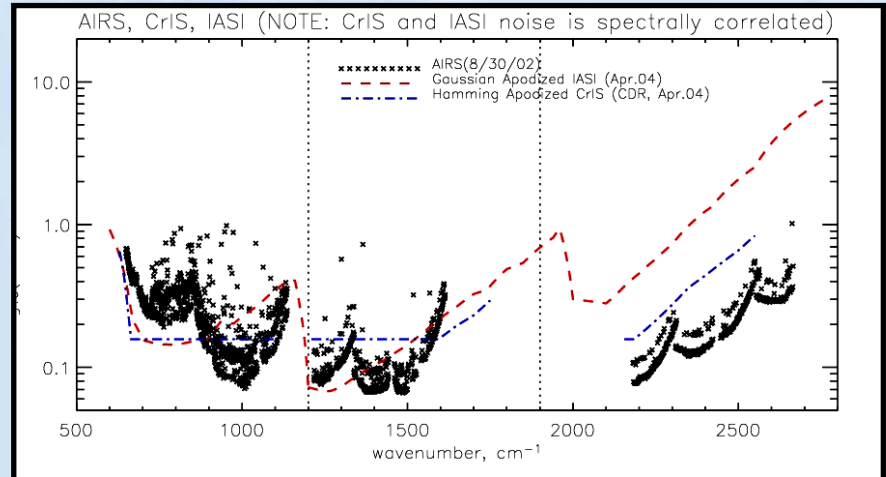
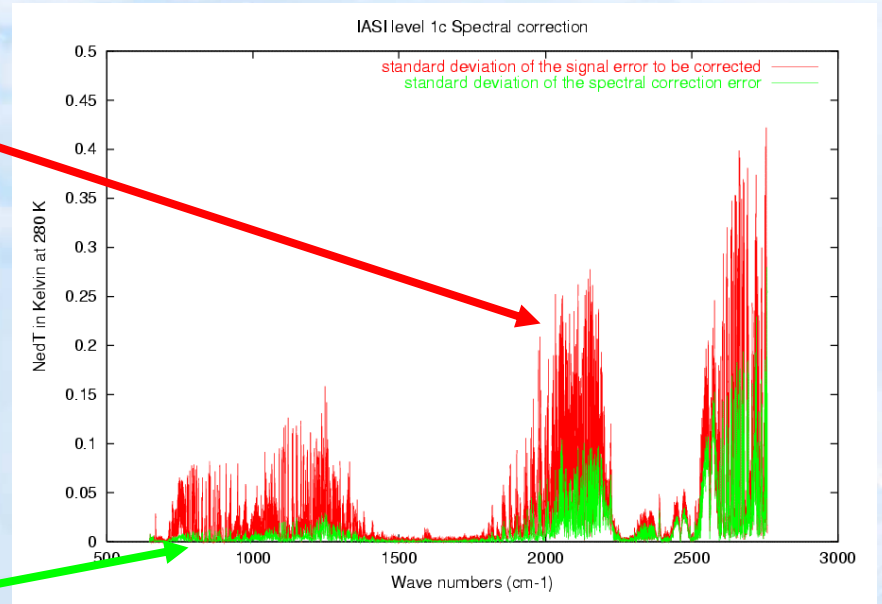
All IASI FOV's have the same OPD (in an ideal world)

Since optical path difference defines ILS and spectral resolution the FOV ILS is an integration of the sub-pixel ILS's weighted by the scene temperature. Therefore ILS becomes a function of clouds and surface.



Sub-pixel ILS Issue Requires Complex RTA Corrections

- Uncorrected IASI spectra will have an additional noise proportional to cloudiness of the scene (red curve in upper right).
- Error induce by computed ILS derived from IASI's sub-pixel imager (32x32 pixels) shown in green.
- NOTE: CrIS does not have built in imager – will rely on VIIRS.
- Random noise is shown in lower right.





Remote Sounding (24 slides)

(continued from yesterday)

The physical approach to derive
geophysical products from
satellite radiances

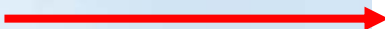


Physical Retrieval is a Minimization of a Cost Function

Covariance of observed minus computed radiances: includes instrument noise model and spectral spectroscopic sensitivity to components of the state, X , that are held constant (Physics *a-priori* spectral information).

$$J = \left(R_n^{obs} - R_n \left(X_j^{i-1} \right) \right)^T \cdot N_{n,n}^{-1} \cdot \left(R_n^{obs} - R_n \left(X_j^{i-1} \right) \right) + \left(X_j^{i-1} - X_j^A \right)^T \cdot C_{j,j}^{-1} \cdot \left(X_j^{i-1} - X_j^A \right)$$

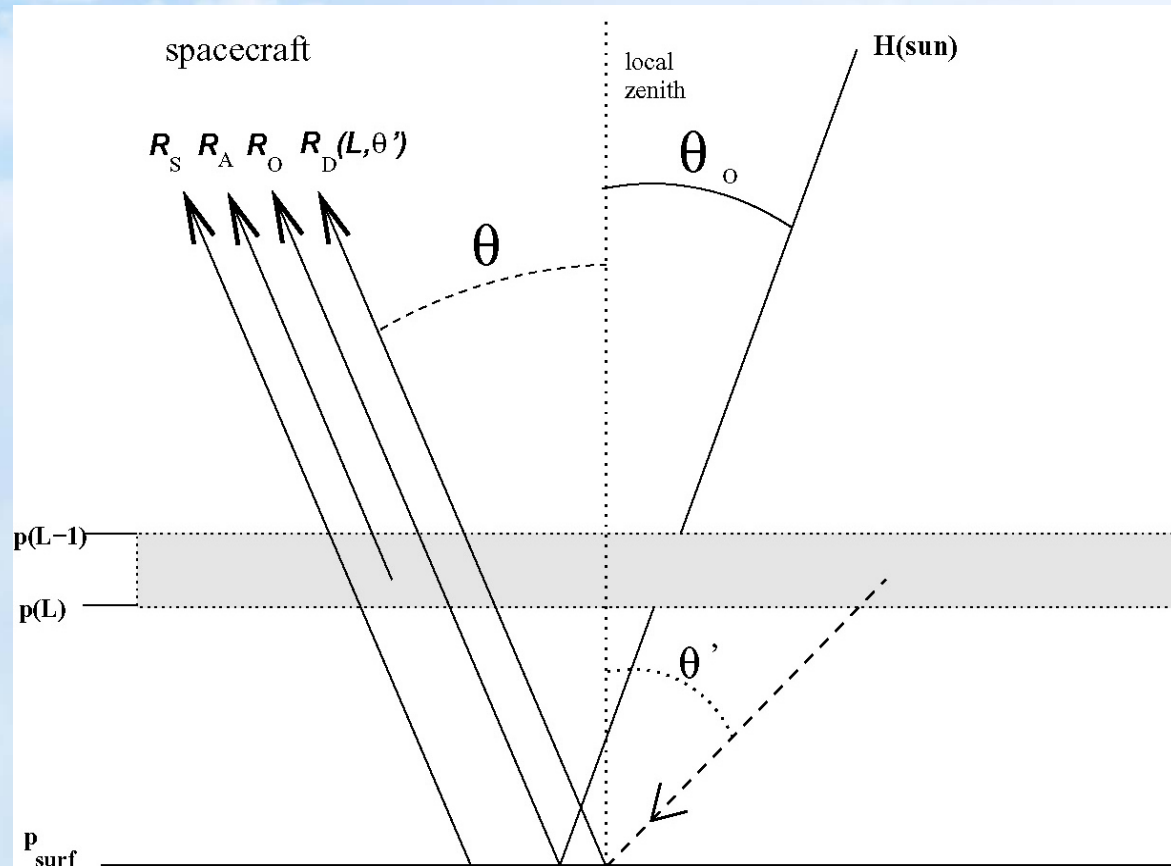
Covariance of products (*e.g.*, T(p), q(p), CO₂(t)) can be used to optimize minimization of this underdetermined problem. Need to decide how much *a-priori* statistics is desired in the product. For climate products one can use a minimum variance approach ($C = \lambda I$) to eliminate inducing correlations. For weather, geophysical correlations (model statistics) are most likely desired.

Derivative of the forward model is required to minimize J. 

$$K_{n,j}^{i-1} = \frac{\partial R_n \left(\vec{X}^{i-1} \right)}{\partial X_j}$$

Radiance at the Satellite is Composed of Many Terms

- Surface Radiance, R_S
- Up-welling Radiance, R_A
- Direct Solar radiance, R_O
- Down-welling Reflected Radiance, R_D
- Scattering (not shown) is composed of reflections radiance from particles within the atmosphere.
- Multiple scattering (not shown) is reflections between particles.



In microwave and clear (or cloud cleared) infrared scenes scattering is negligible.



Thermal Sounder Forward Model

Example: Upwelling Radiance Term

Each channel samples a finite spectral region

Absorption coefficients, κ , for any spectrally active molecular species, i , (e.g., water, ozone, CO, etc.) must be computed.

κ is also a strong function of pressure, temperature, and interactions between species.

$$R_n(\vec{X}) \simeq \int_{\nu} \Phi_n(\nu) \int_p B_{\nu}(T(p)) \cdot \frac{\partial \exp \left(- \int_{z'=\infty}^{z(p)} \sum_i \kappa_i(\vec{X}, p, \dots) dz' \right)}{\partial p} \cdot dp \cdot d\nu$$

Inversion of this equation is highly non-linear and under-determined.

Vertical temperature gradient is critical for thermal sounding.

Full radiative transfer equation includes surface, down-welling, and solar reflection terms.

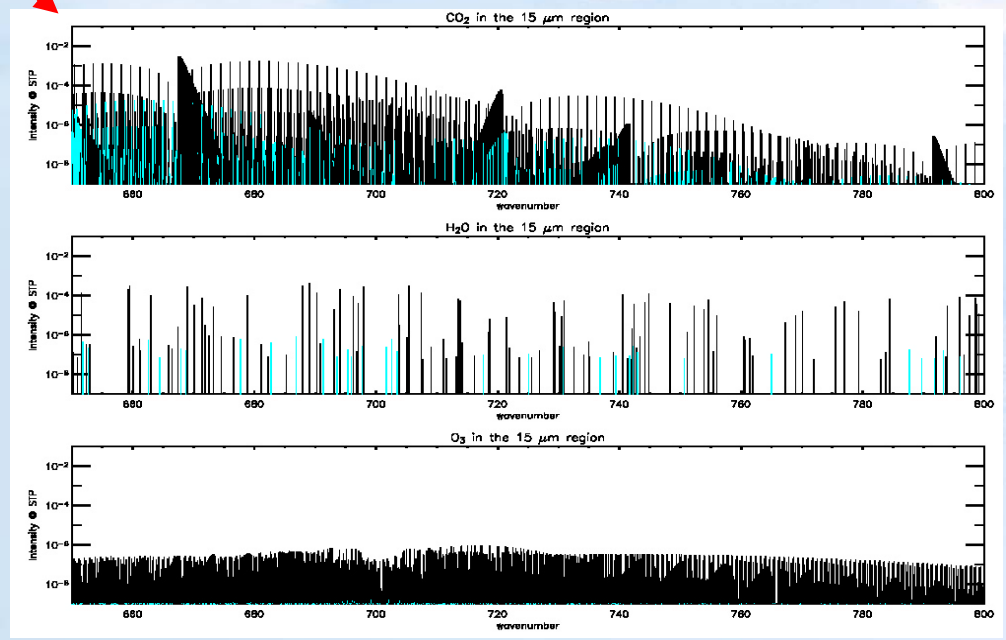
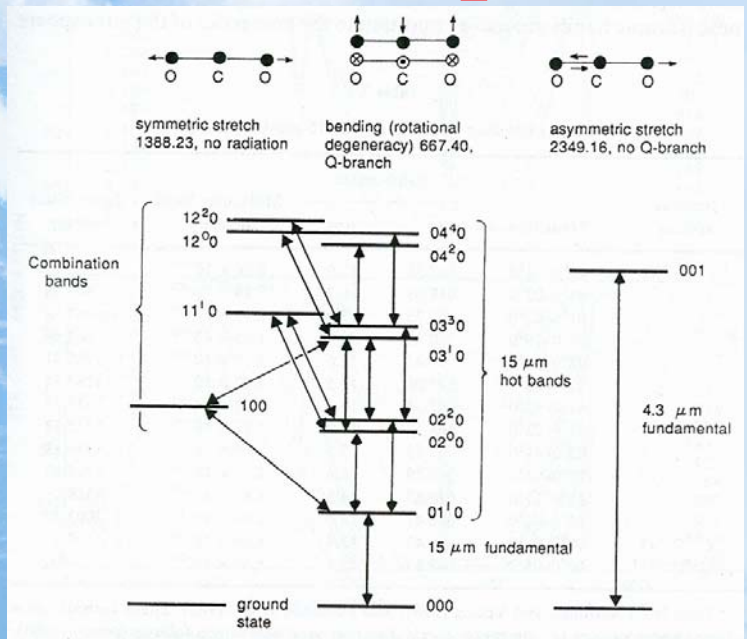


All the Physics is Contained in the Absorption Coefficient

- The absorption coefficient is a complicated and highly non-linear function
- Line Strengths, S_{ij} , result from many molecular vibrational-rotational transitions.

$$\kappa_i(\nu, p, T, \theta) \simeq \sum_{j=1}^J \frac{N_i \cdot S_{ij}}{\pi} \frac{\gamma_{ij}}{(\nu - \nu_{ij})^2 + (\gamma_{ij})^2} \cdot \sec(\theta)$$

$$\gamma_{ij} \simeq \gamma_{ij}^0 \cdot \frac{p}{P_0} \cdot \sqrt{\frac{T}{T_0}}$$



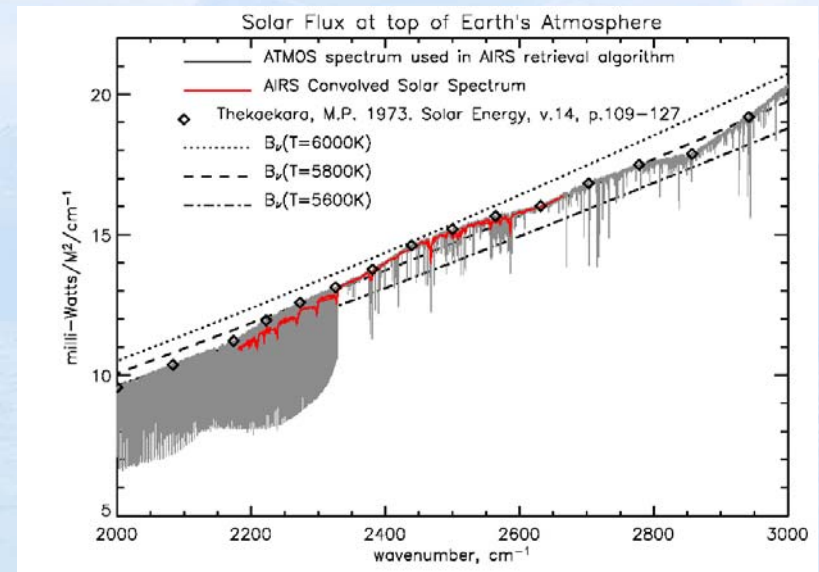
The Solar (or Direct) Term, Without Scattering, is Given by

$$R_{\odot} = \rho_{\odot}(\nu, \theta, \theta_{\odot}) \cdot \tau_{\nu}^{\downarrow\uparrow}(p_s, X, \theta, \theta_{\odot}) \cdot \Omega(t) \cdot H_{\odot}(\nu) \cdot \cos(\theta)$$

$$\Omega(t) = \pi \cdot \left(\frac{0.6951 \cdot 10^9}{D_{\odot}(t)} \right)^2$$

$$\simeq 6.79 \cdot 10^{-5} - 0.23 \cdot 10^{-5} \cdot \cos(2\pi(t - t_0)/t_y)$$

- Source Function, H, is the Solar radiance at 1AU
- $\Omega(t)$ is the ratio of solid angle of the sun as a function of the Earth's orbital distance to reference distance (1 AU).
- Bi-directional transmittance contains all the atmospheric physics
- Surface reflectivity is a strong function of geometry and surface type.



Down-welling Thermal Term

$$R_d(\nu, \theta) = \tau_\nu^\uparrow(P_s, X, \theta) \cdot \int_{\alpha=0}^{2\pi} \int_{\theta'=0}^{\frac{\pi}{2}} \rho_\nu(\theta, \theta', \alpha) \cdot \sin(\theta') \cdot \cos(\theta') \cdot d\theta' \cdot d\alpha \\ \cdot \int_{p=P_s}^0 B_\nu(T(p)) \cdot \frac{d\tau_\nu^\downarrow(p, X, \theta')}{dp} \cdot dp$$

In the microwave we assume the down-welling transmittance is monochromatic and compute a diffuse angle that is a function of surface type. Over ocean the microwave diffusive angle is a function of wind speed and is retrieved.

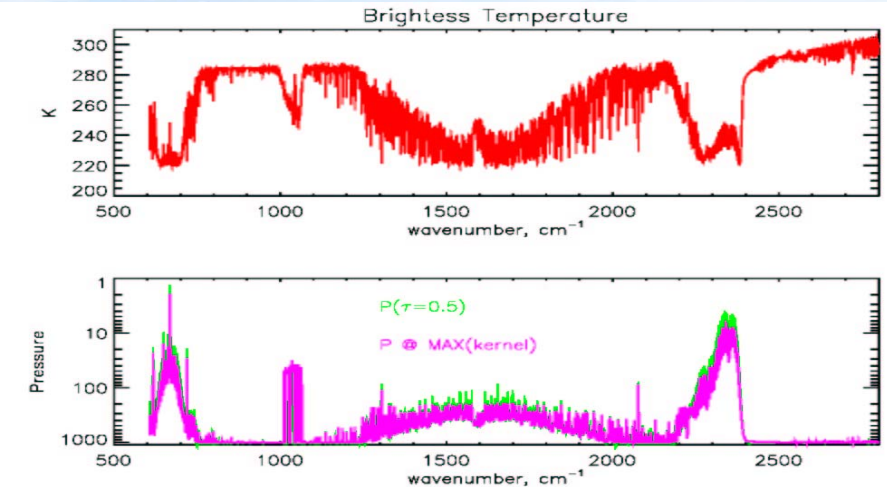
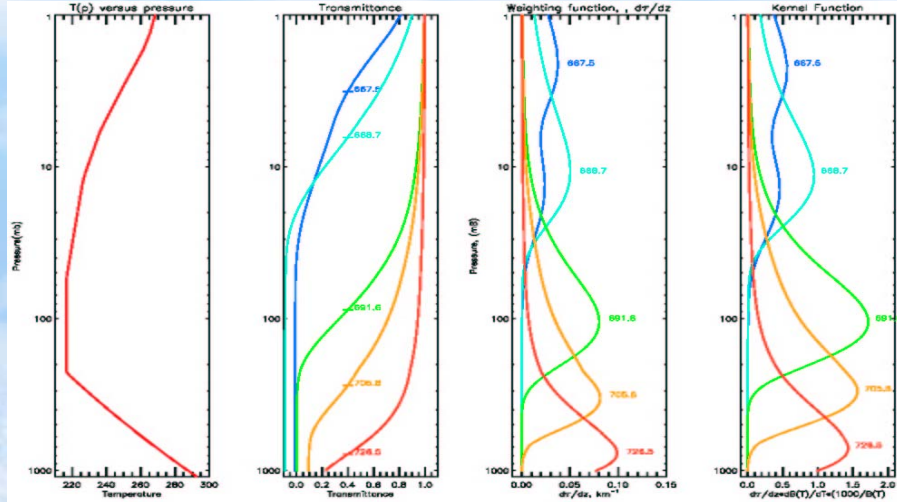
$$\Theta_d(n, \theta) = \tau_\nu^\uparrow(P_s, \theta) \cdot (1 - \epsilon_\nu) \sum_{L=1}^{N_L} \left[\overline{T(L)} \cdot \Delta\tau_\nu^\downarrow(L, \theta) \right]$$

$$\Delta\tau_\nu^\downarrow(L, \theta) \simeq \left(\frac{\tau_\nu^\uparrow(P_{surf}, \theta)}{\tau_\nu^\uparrow(p(L), \theta)} \right)^f - \left(\frac{\tau_\nu^\uparrow(P_{surf}, \theta)}{\tau_\nu^\uparrow(p(L-1), \theta'_\nu)} \right)^f$$

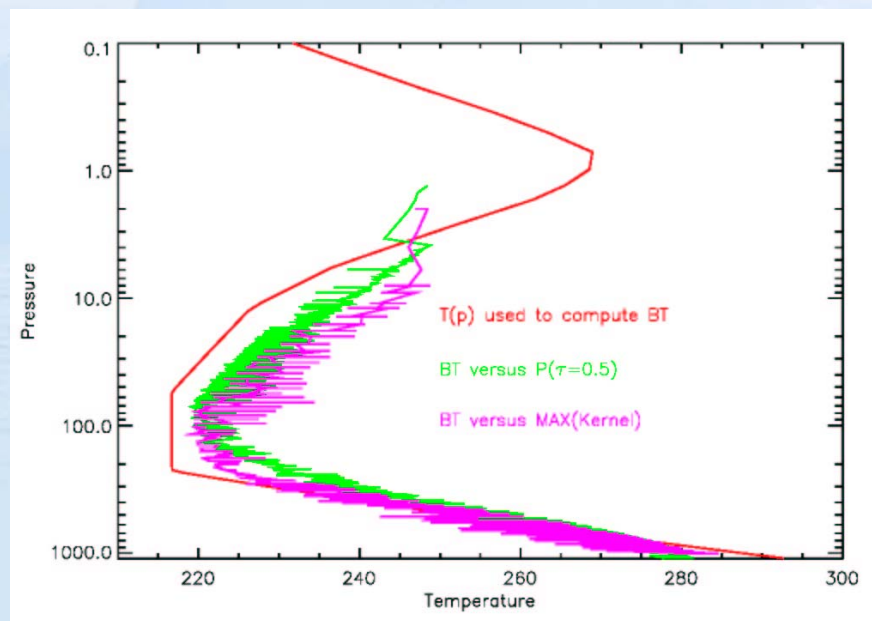
f = ratio of secant angles



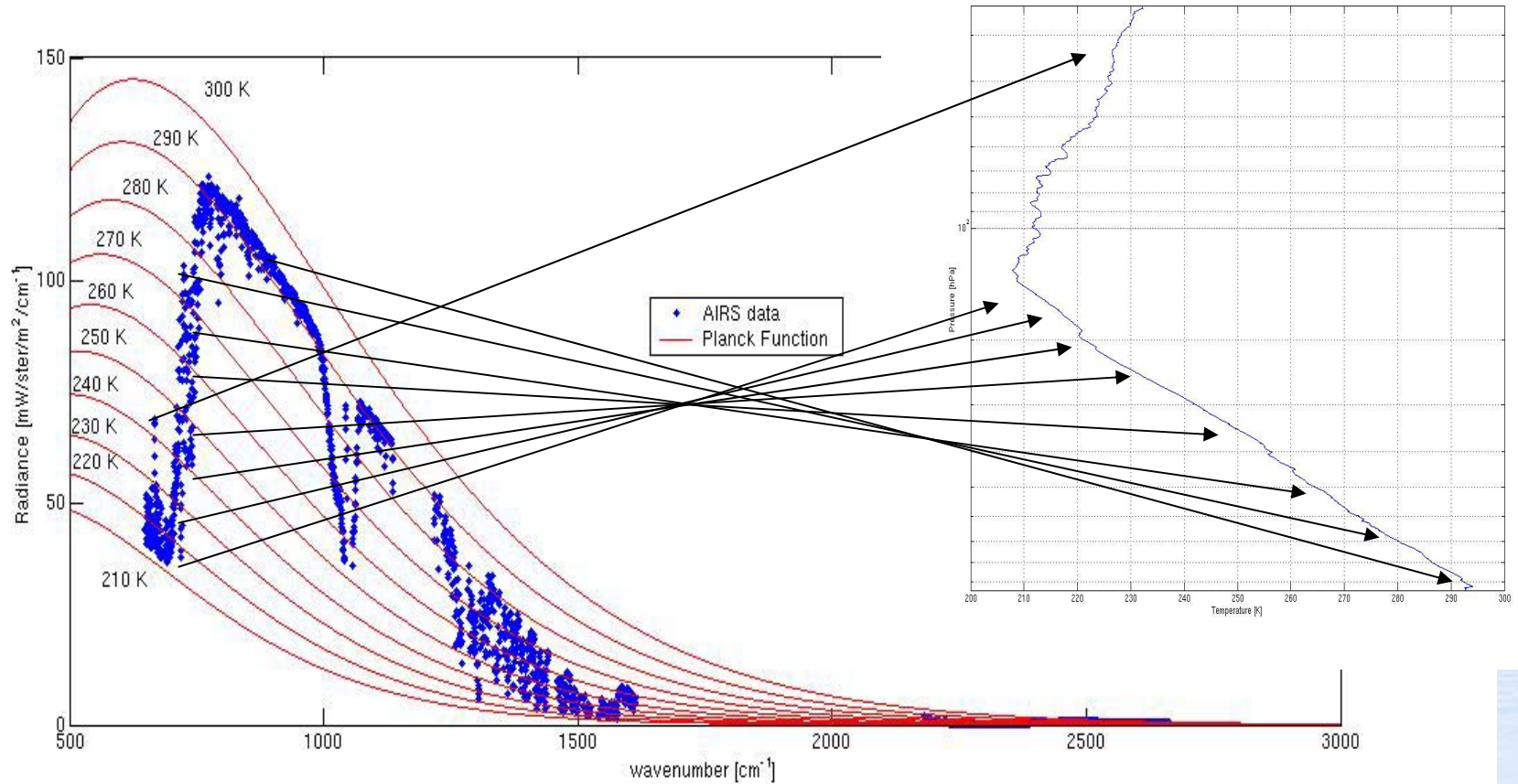
Physics Knowledge is What Allows Interpretation of Spectra



- Given an estimate of the atmospheric state we can compute transmittance.
- Weighting functions, $dR/d\tau$, determine where transmittance changes quickly.
- Kernel functions, K , includes effect of lapse rate on a channels sensitivity.
- If we map measured brightness temperature to altitude of sensitivity we can get a reasonable estimate of the temperature profile directly from the spectrum.



The Advantage of High Spectral Resolution is Vertical Resolution



Sampling over rotational bands

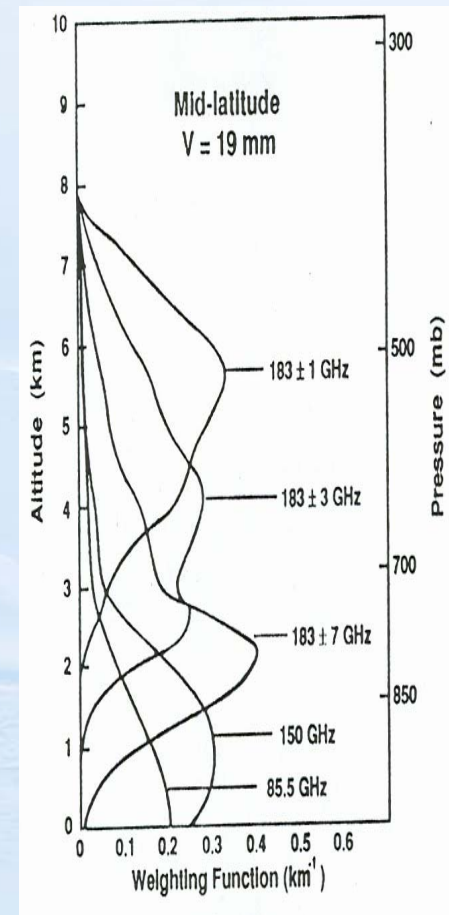
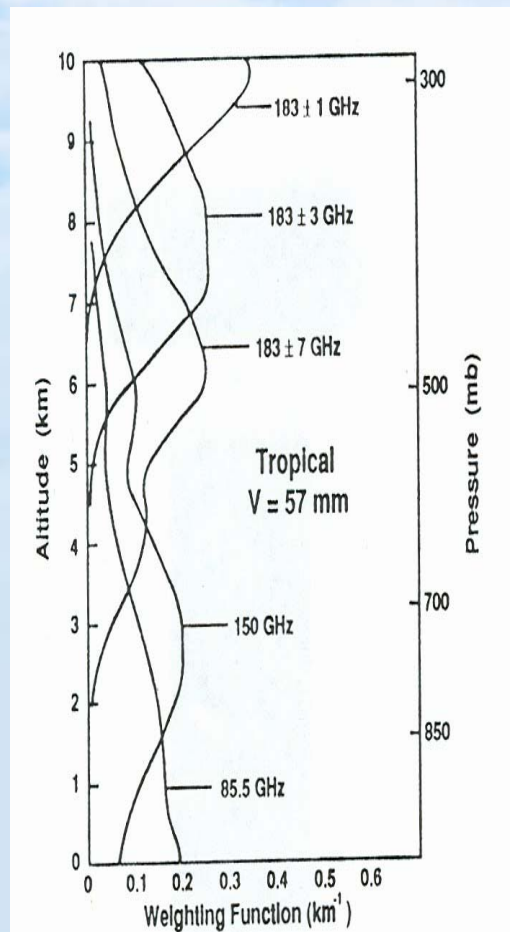
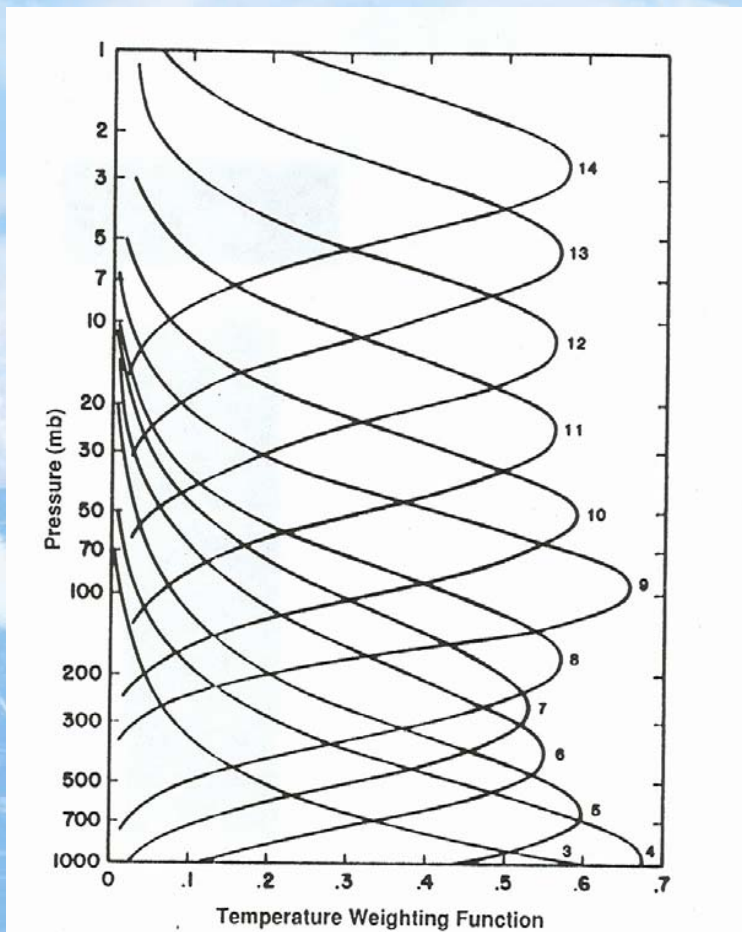


AMSU Temperature & Moisture Channel Weighting Functions

$$W = d\tau/dz$$

$$W = d\tau/dq \text{ tropical}$$

$$W = d\tau/dq \text{ mid-lat}$$



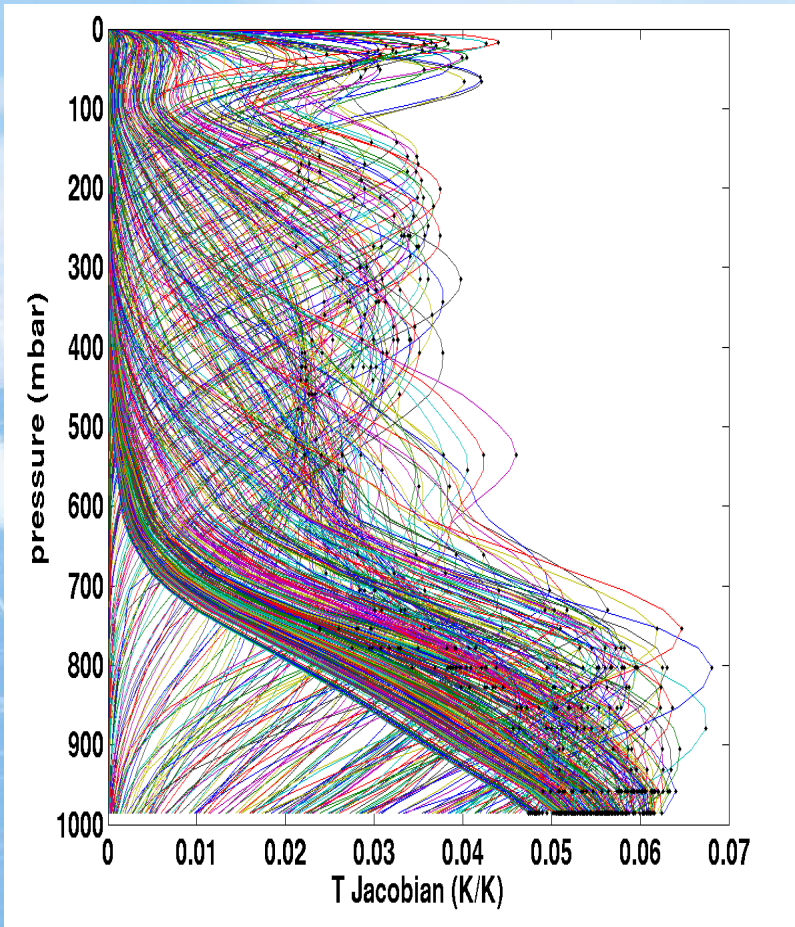
$K = dB_{\nu}(t)/dT * d\tau/dz$, Figures from M.A. Janssen 1993 John Wiley & Sons



Example Channel Kernel Functions, $K_{n,j}$ for Temperature and Moisture

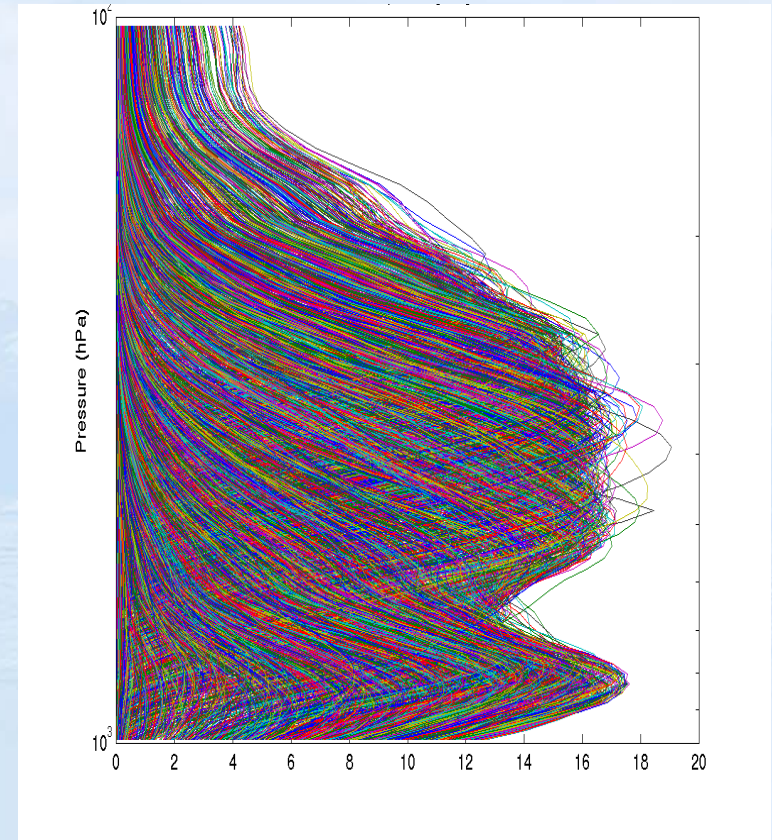
AIRS 15 μm (650-800 cm^{-1}) band

$$K = dR/dT$$



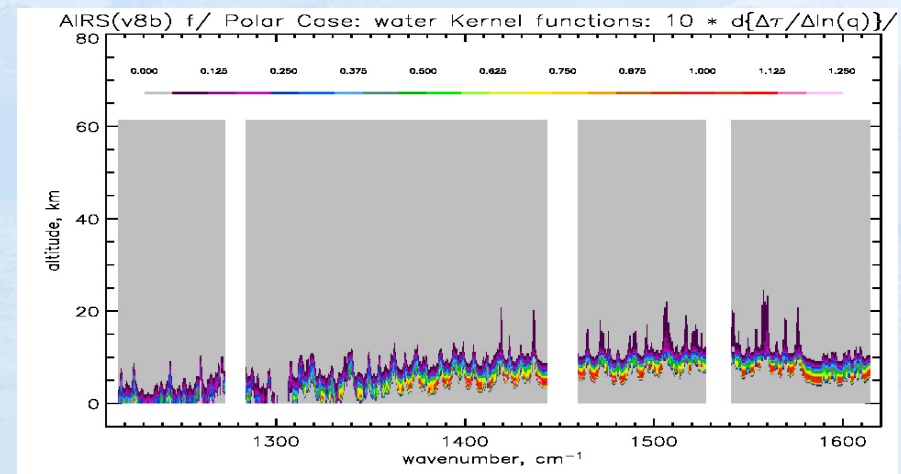
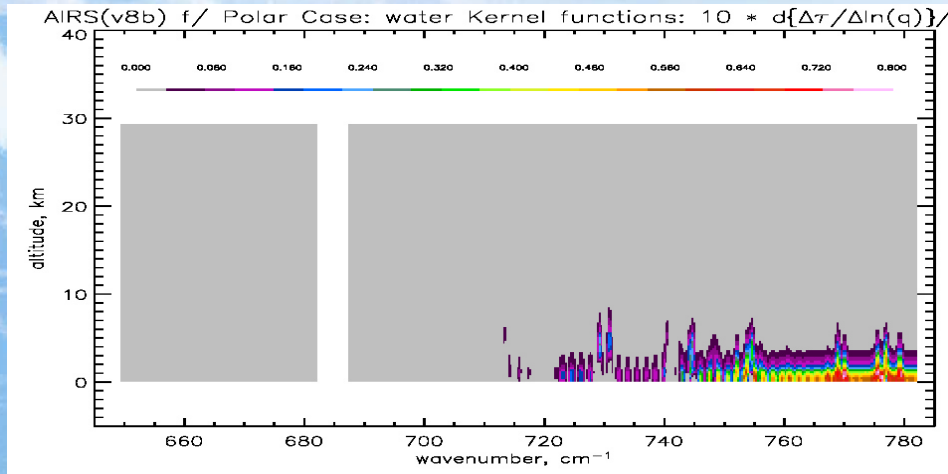
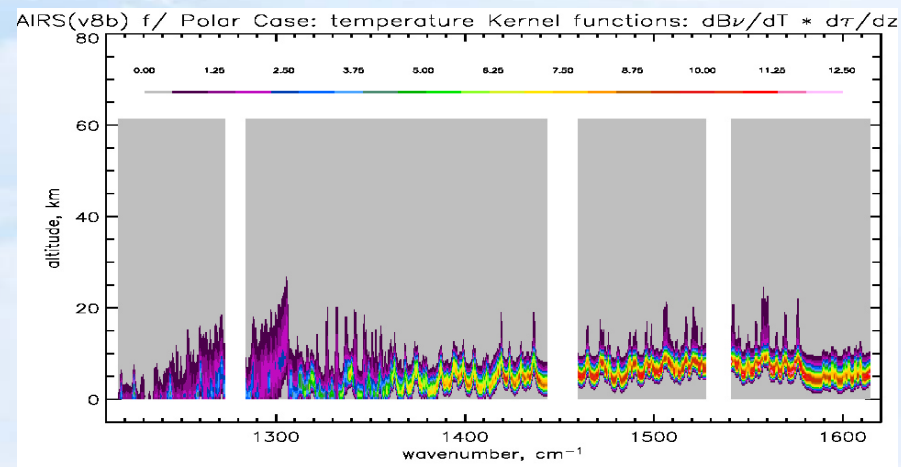
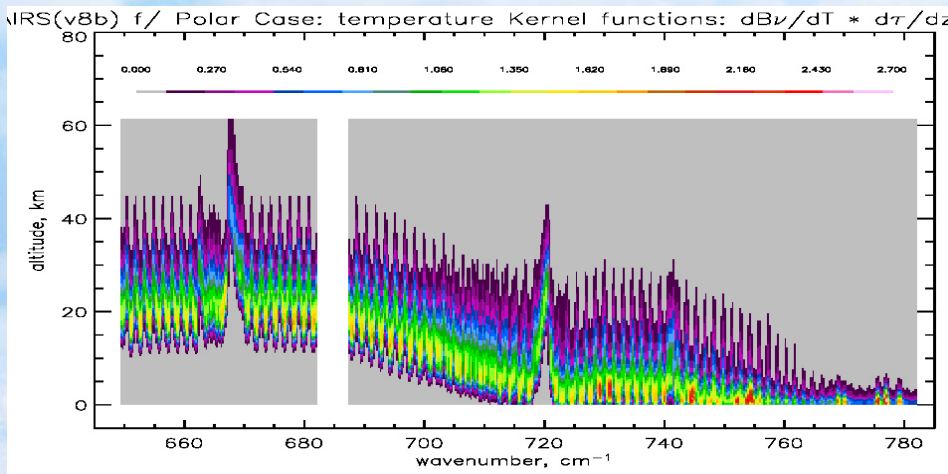
AIRS 6.7 μm (1200-1600 cm^{-1}) band

$$K = dR/dq$$

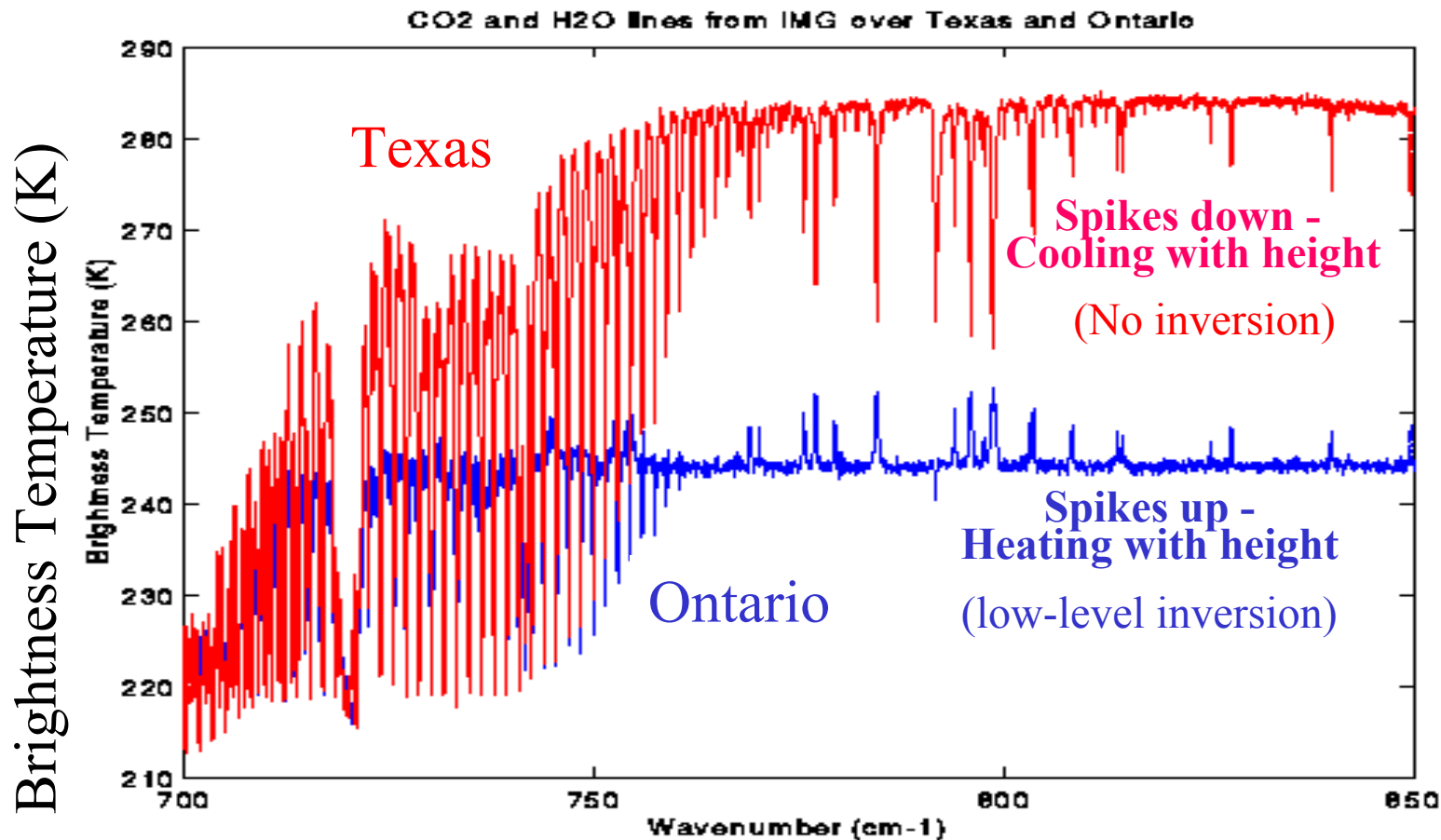




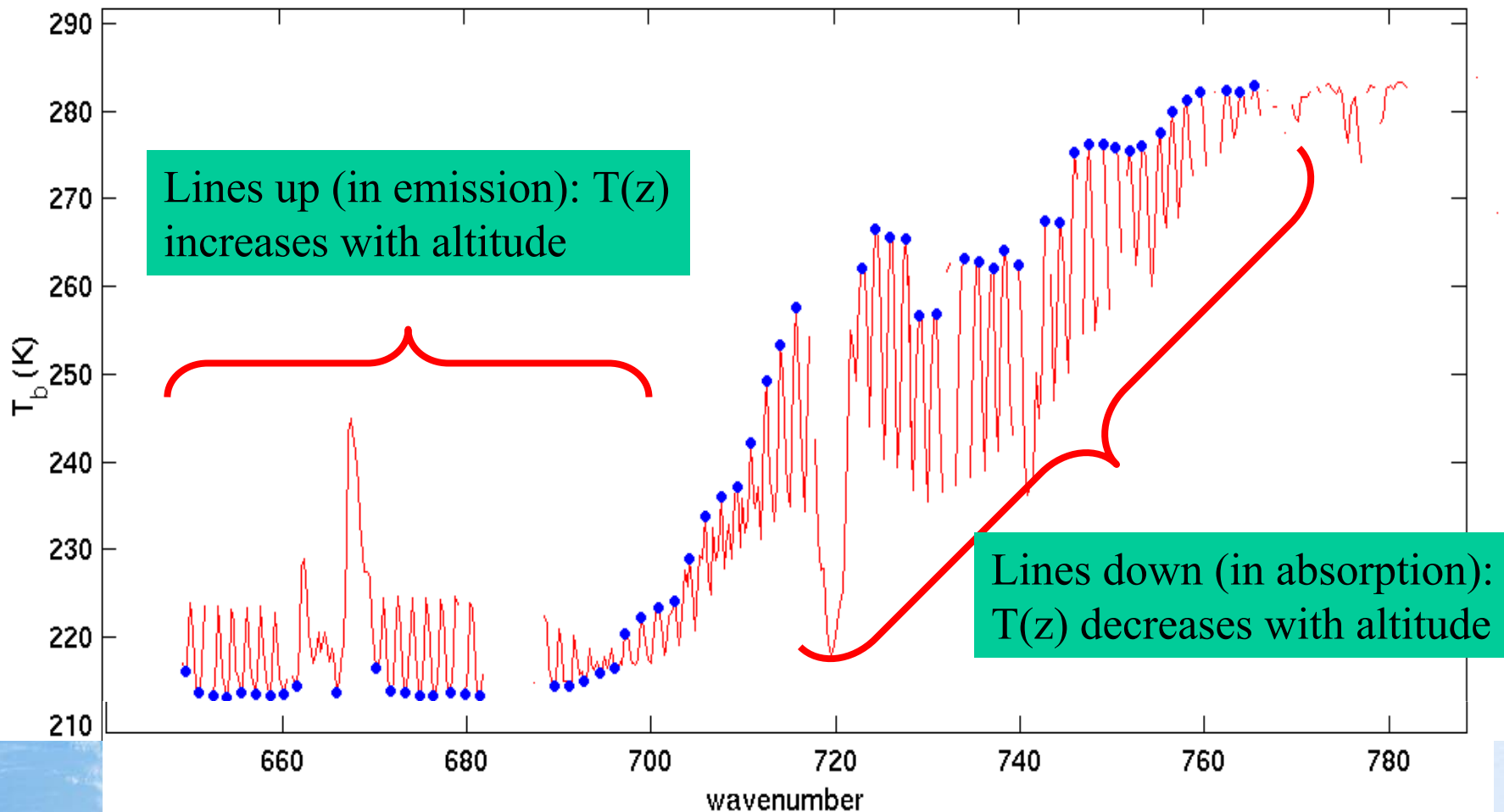
AIRS (v8b) f/ Polar Case: temperature Kernel functions: $dB\nu/dT * d\tau/dz$ and Moisture Channel Kernel Functions



Weak Lines (Water & CO₂) in Window Region Sound Boundary Layer Inversions



Example of 15 μm Spectrum with “in-between” the Lines Marked with Blue Dots




The Inverse Solution: Low Resolution Instruments

$$\Delta X_j = [K_{j,n}^T \cdot N_{n,n}^{-1} \cdot K_{n,j} + C_{j,j}^{-1}]^{-1} \cdot [K_{j,n}^T \cdot N_{n,n}^{-1} \cdot \Delta R_n + C_{j,j}^{-1} \cdot \Delta X_j^a]$$

Measurement
Covariance

Constraint

Weighted Average of
Observations & *a-priori*



Traditional methods (Rodgers, Eyre, etc) had to rely on the statistics of the *a-priori* term (*models, climatologies, etc*) due to lack of information from the measurements (HIRS/MSU had 23 sounding channels).

The Inverse Solution: Hyper-spectral Instruments

$$\Delta X_j = \left[K_{j,n}^T \cdot N_{n,n}^{-1} \cdot K_{n,j} + C_{j,j}^{-1} \right]^{-1} \cdot \left[K_{j,n}^T \cdot N_{n,n}^{-1} \cdot \Delta R_n + C_{j,j}^{-1} \cdot \Delta X_j^a \right]$$

- **AIRS: 2378 channels**
- **IASI: 8461 channels**

Hyper spectral Instruments measurements have much higher information content:

 ***AIRS inverse method exploits the high information content of the instrument & a-priori information in the radiative physics without a penalty in execution time.***

Iterative Solution to the Cost Function has many forms

- Optimal estimation can “pivot” off of the *a-priori* state.

$$\mathbf{X}_j^i = \mathbf{X}_j^A + \left[\mathbf{K}_{j,n}^T \cdot \mathbf{N}_{n,n}^{-1} \cdot \mathbf{K}_{n,j} + \mathbf{C}_{j,j}^{-1} \right]^{-1} \cdot \mathbf{K}_{j,n}^T \cdot \mathbf{N}_{n,n}^{-1} \cdot \left[\mathbf{R}_n^{obs} - \mathbf{R}_n(\mathbf{X}^{i-1}) + \mathbf{K}_{n,j} \cdot (\mathbf{X}_j^{i-1} - \mathbf{X}_j^A) \right]$$

- Equivalent to “pivoting” from the previous iteration:

$$\mathbf{X}_j^i = \mathbf{X}_j^{i-1} + \left[\mathbf{K}_{j,n}^T \cdot \mathbf{N}_{n,n}^{-1} \cdot \mathbf{K}_{n,j} + \mathbf{C}_{j,j}^{-1} \right]^{-1} \cdot \left[\mathbf{K}_{j,n}^T \cdot \mathbf{N}_{n,n}^{-1} \cdot (\mathbf{R}_n^{obs} - \mathbf{R}_n(\mathbf{X}^{i-1})) - \mathbf{C}_{j,j}^{-1} \cdot (\mathbf{X}_j^{i-1} - \mathbf{X}_j^A) \right]$$

- The **background term**, modifies obs-calc’s to converge to a regularized solution. Form used in our algorithm:

$$\mathbf{X}_j^i = \mathbf{X}_j^{i-1} + \left[\mathbf{K}_{j,n}^T \cdot \mathbf{N}_{n,n}^{-1} \cdot \mathbf{K}_{n,j} + \mathbf{H}_{j,j} \right]^{-1} \cdot \mathbf{K}_{j,n}^T \cdot \mathbf{N}_{n,n}^{-1} \cdot \left[\mathbf{R}_n^{obs} - \mathbf{R}_n(\mathbf{X}^{i-1}) - \Psi_n^{i-1} \right]$$

The cost function minimizes differences between observations and computed radiances

$$R_n^{obs} - R_n(\vec{X}) \simeq K_{n,j} \cdot \Delta \vec{X}_j + \epsilon_n$$

- Linear minimization of cost function is equivalent to expanding Obs-calc's into a Taylor expansion and minimizing with constrained LSQ fitting.
- In a linear operator, the different components of geophysical space can be separated.

$$\begin{aligned}
 R_n^{obs} - R_n(\vec{X}) &\simeq K_{n,i}^1 \cdot \Delta \vec{T}_i \\
 &+ K_{n,i}^2 \cdot \Delta \vec{q}_i \\
 &+ K_{n,i}^3 \cdot \Delta \vec{O}_i \\
 &+ K_{n,i}^4 \cdot \Delta \vec{C}O_i \\
 &+ \dots + \epsilon_n
 \end{aligned}$$

$$K_{n,j} = \frac{\partial R_n(\vec{X})}{\partial X_j}$$



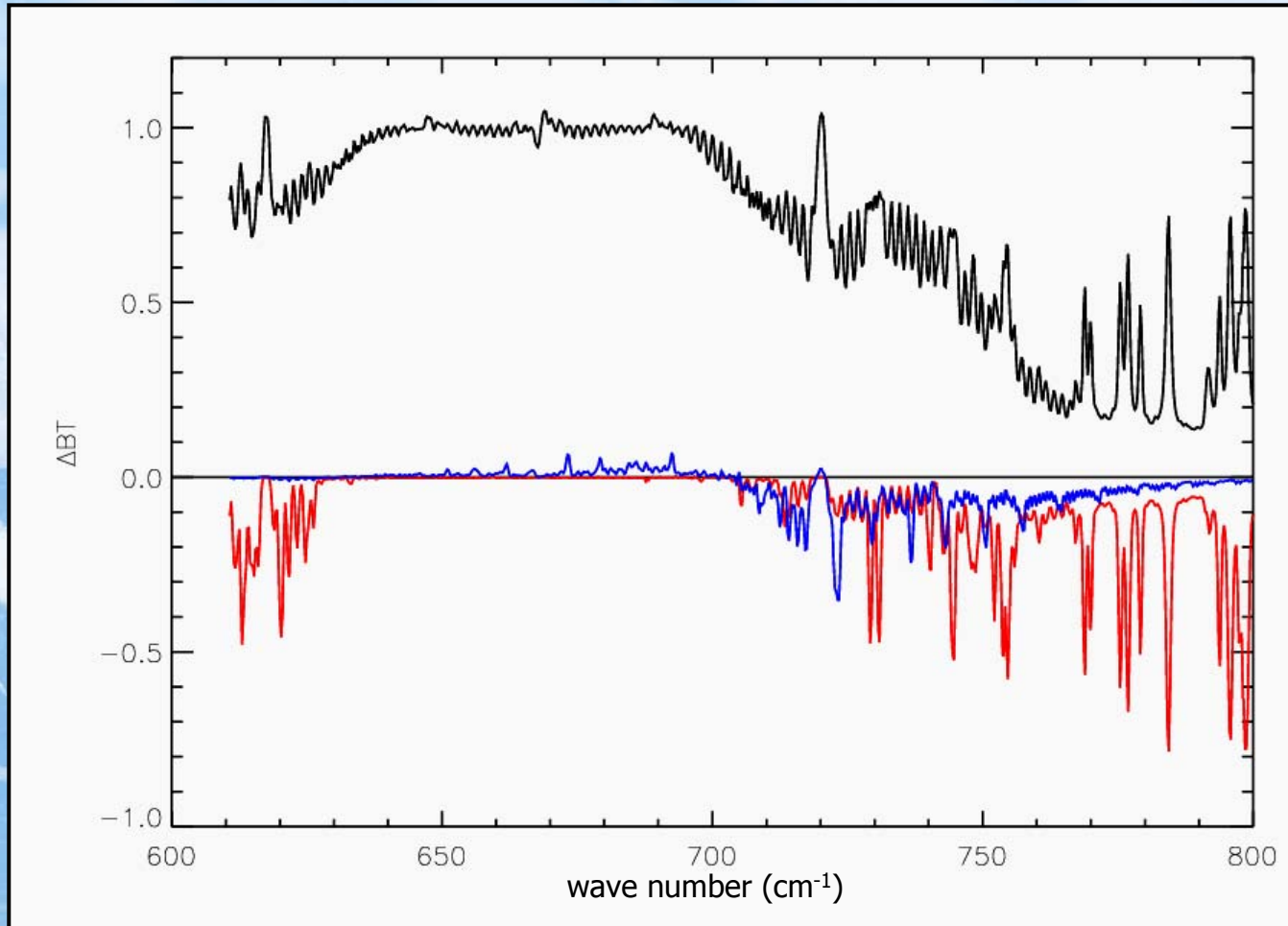
The Problem is Physical and Can be Solved by Parts

$$R_n^{obs} - R_n(\vec{X}) \simeq K_{n,i}^1 \cdot \Delta \vec{T}_i + e_n$$

- Careful analysis of the physical spectrum will show that many components are physically separable (spectral derivatives are unique)
- Select channels within each step with large K and small e_n
- This makes solution more stable.
- And has significant implications for operational execution time.

$$\begin{aligned} e_n &= K_{n,i}^2 \cdot \delta \vec{q}_i \\ &+ K_{n,i}^3 \cdot \delta \vec{O}_i \\ &+ K_{n,i}^4 \cdot \delta \vec{C}O_i \\ &+ \dots + \epsilon_n \end{aligned}$$

Sensitivity Analysis for Temperature Retrieval in 15 μm Band



**1K temperature
perturbation**

**10% water
perturbation**

**10% ozone
perturbation**

Step 1: *Temperature Solution*

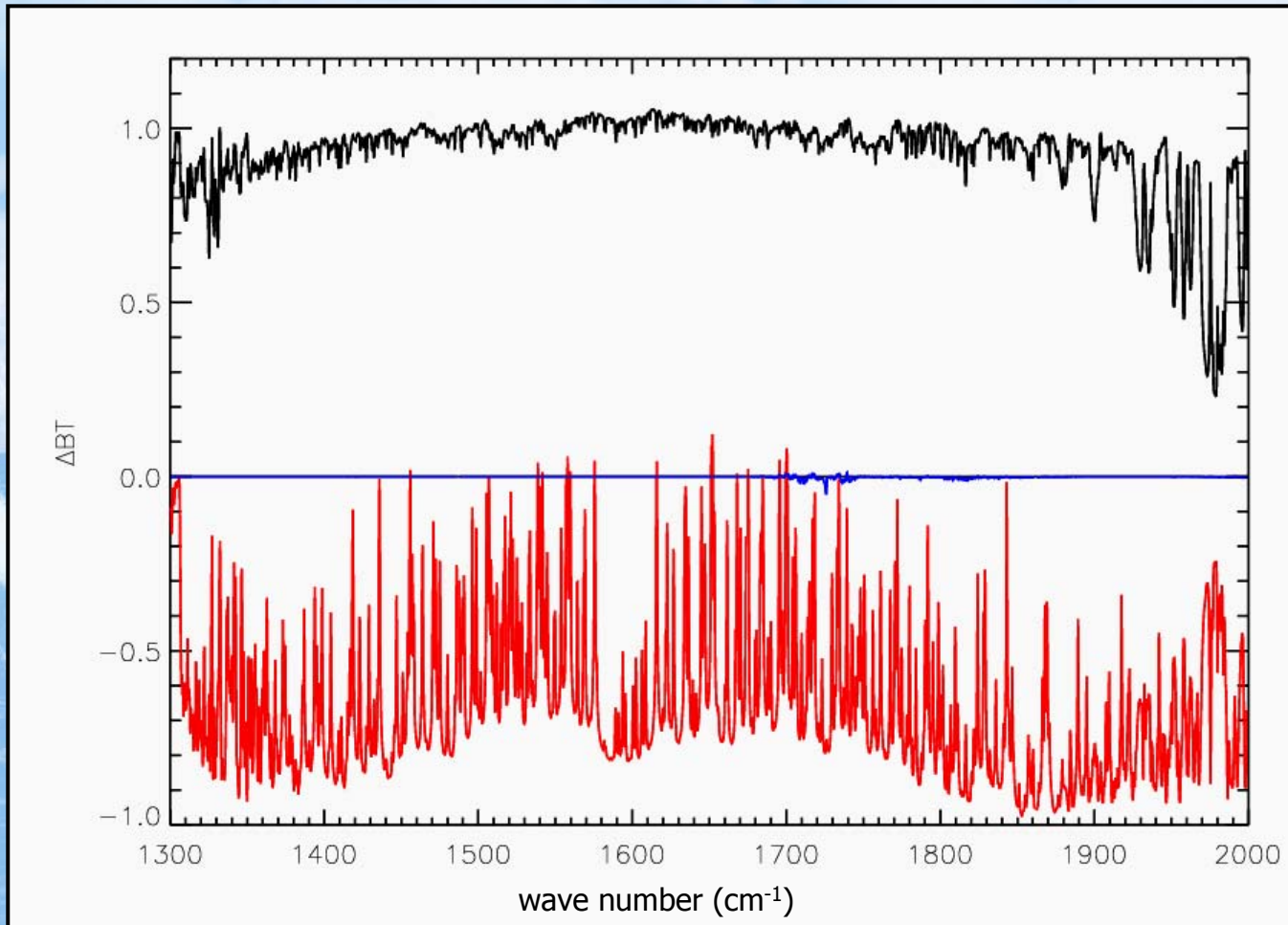
$$R_n^{obs} - R_n(\vec{X}) \approx K_{n,i}^1 \cdot \Delta T_i + e_n$$

$$e_n = K_{n,i}^2 \cdot \delta \vec{q}_i + K_{n,i}^3 \cdot \delta \vec{O}_{3i} + K_{n,i}^4 \cdot \delta \vec{CO}_i + \dots + \varepsilon_n$$

$$\Delta T_i = [K_{i,n}^{1T} \cdot N_{n,n}^{-1} \cdot K_{i,n}^1 + C_{i,i}^{-1}]^{-1} \cdot [K_{i,n}^{1T} \cdot N_{n,n}^{-1} \cdot \Delta R_n + C_{i,i}^{-1} \cdot \Delta T_i^a]$$

$$N = \delta R_{CCR} \delta R_{CCR}^T + K^2 \delta q \delta q^T K^{2T} + K^3 \delta O_3 \delta O_3^T K^{3T} + \dots$$

Sensitivity Analysis for Water Vapor Retrieval in 6.7 μm Band



**1K temperature
perturbation**

**10% water
perturbation**

**10% ozone
perturbation**

Step 2: *Water Vapor Solution*

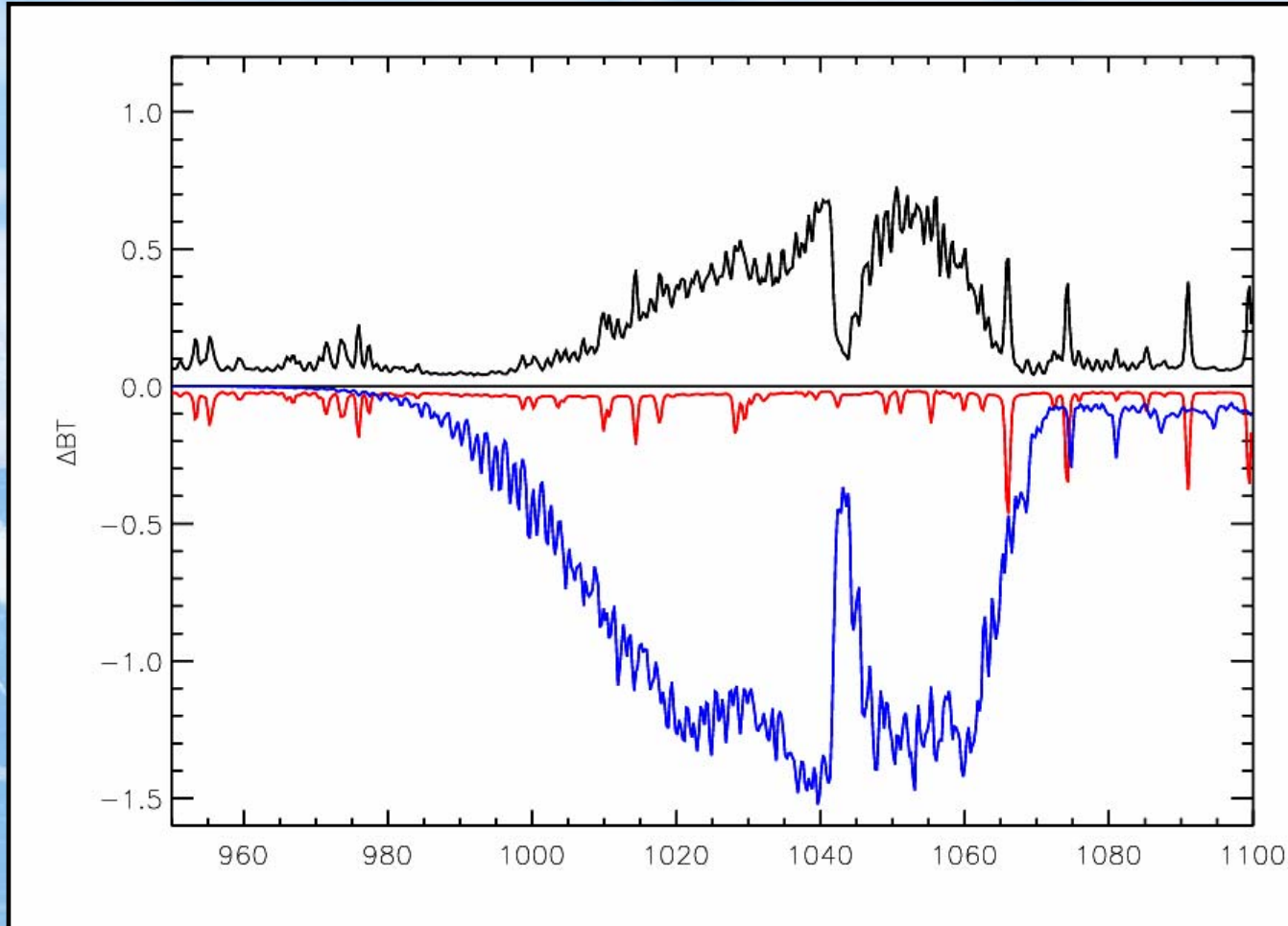
$$R_n^{obs} - R_n(\vec{X}) \approx K_{n,i}^2 \cdot \Delta \vec{q}_i + e_n$$

$$e_n = K_{n,i}^1 \cdot \delta \vec{T}_i + K_{n,i}^3 \cdot \delta \vec{O}_{3i} + K_{n,i}^4 \cdot \delta \vec{CO}_i + \dots + \varepsilon_n$$

$$\Delta q_i = [K_{i,n}^{2T} \cdot N_{n,n}^{-1} \cdot K_{i,n}^2 + C_{i,i}^{-1}]^{-1} \cdot [K_{i,n}^{2T} \cdot N_{n,n}^{-1} \cdot \Delta R_n + C_{i,i}^{-1} \cdot \Delta q_i^a]$$

$$N = \delta R_{CCR} \delta R_{CCR}^T + K^1 \delta T \delta T^T K^{1T} + K^3 \delta O_3 \delta O_3^T K^{3T} + \dots$$

Sensitivity Analysis for Ozone Retrieval in 9.6 μm Band



**1K temperature
perturbation**

**10% water
perturbation**

**10% ozone
perturbation**

Step 3: Ozone Solution

$$R_n^{obs} - R_n(\vec{X}) \approx K_{n,i}^3 \cdot \Delta \vec{O}_{3i} + e_n$$

$$e_n = K_{n,i}^1 \cdot \delta \vec{T}_i + K_{n,i}^2 \cdot \delta \vec{q}_i + K_{n,i}^4 \cdot \delta \vec{CO}_i + \dots + \varepsilon_n$$

$$\Delta O_{3i} = [K_{i,n}^{3T} \cdot N_{n,n}^{-1} \cdot K_{i,n}^3 + C_{i,i}^{-1}]^{-1} \cdot [K_{i,n}^{3T} \cdot N_{n,n}^{-1} \cdot \Delta R_n + C_{i,i}^{-1} \cdot \Delta O_{3i}^a]$$

$$N = \delta R_{CCR} \delta R_{CCR}^T + K^1 \delta T \delta T^T K^{1T} + K^2 \delta q \delta q^T K^{2T} + \dots$$